ELSEVIER

MCN Molecular and Cellular Neuroscience

www.elsevier.com/locate/ymcne
Mol. Cell. Neurosci. 25 (2004) 205–216

Identification of two *nogo/rtn4* genes and analysis of Nogo-A expression in *Xenopus laevis*☆

Michael Klinger,[a,1] Heike Diekmann,[a,1] Dietmar Heinz,[a] Cordula Hirsch,[a] Sylvia Hannbeck von Hanwehr,[a] Barbara Petrausch,[a] Thomas Oertle,[b] Martin E. Schwab,[b] and Claudia A.O. Stuermer[a,*]

[a] *Department of Biology, University of Konstanz, 78457 Konstanz, Germany*
[b] *Department of Biology, ETH Zurich and Brain Research Institute, University of Zurich, 8057 Zurich, Switzerland*

Received 5 August 2003; revised 15 September 2003; accepted 29 September 2003

Myelin-associated axon growth inhibitors such as Nogo-A/RTN4-A impair axon regeneration in the adult mammalian central nervous system (CNS). Here, we describe the cloning and expression of two independent *Xenopus laevis rtn4* orthologs. As in mammals, alternative transcripts are generated both through differential splicing and promoter usage, giving rise to *Xenopus* nogo-A, -B, -C and to a new isoform, nogo-N/rtn4-N. *Xenopus* is therefore the 'lowest' vertebrate where Nogo-A was identified.

***Xenopus* Nogo-A/RTN4-A is predominantly expressed in the nervous system, whereas the other isoforms mainly occur in non-neuronal tissues. Nogo-A/RTN4-A specific antisera detect the protein in myelinated fiber tracts of the spinal cord, hindbrain, optic nerve, tectum opticum and in isolated oligodendrocytes. In addition, subpopulations of CNS neurons are Nogo-A/RTN4-A positive. This expression pattern is consistent with that observed for rat Nogo-A and suggests similar functions. Nogo-A in *Xenopus* myelin might therefore contribute to the failure of spinal cord regeneration in frogs—a feature that may have evolved during the transition from fish to land vertebrates.**

Introduction

In the adult mammalian and avian central nervous systems (CNS), regeneration of lesioned nerve fibers is prevented by inhibitory proteins that are particularly enriched in myelin and oligodendrocytes (Caroni and Schwab, 1988b), such as myelin-associated glycoprotein (MAG) (McKerracher et al., 1994), oligodendrocyte-myelin glycoprotein (OMgp) (Wang et al., 2002a) and Nogo/RTN4 (Chen et al., 2000; GrandPré et al., 2000; Prinjha et al., 2000). Earlier functional studies indicated the presence of related neurite growth inhibitors, in particular the IN-1 antigen, in oligodendrocytes/CNS myelin of *Xenopus* (Lang et al., 1995). The IN-1 antibody has originally been raised against a 250 kDa myelin fraction (Caroni and Schwab, 1988a), and based on its neutralizing activity the bovine Nogo-A ortholog (bNI220) has been purified (Spillmann et al., 1998).

Nogo/RTN4 is a member of the reticulon (RTN) family of proteins (Chen et al., 2000; GrandPré et al., 2000; Prinjha et al., 2000). These proteins share a conserved 188 amino acid (aa) long C-terminal reticulon homology domain (RHD) (Oertle et al., 2003b). The two hydrophobic stretches within the RHD could serve as transmembrane domains for their insertion in endoplasmic reticulum (ER) and plasma membranes (Oertle et al., 2003c; van de Velde et al., 1994). Outside the RHD domain, Nogo/RTN4 and the other three RTN proteins (RTN1-3) have no obvious sequence similarities.

In mammals, the *nogo/rtn4* gene gives rise to different isoforms both through alternative splicing and alternative promoter usage with the three major transcripts known as nogo-A, nogo-B and nogo-C (Oertle et al., 2003a). The largest isoform, Nogo-A/RTN4-A, has been described as a potent neurite growth inhibitor of CNS myelin with two inhibitory sites. A stretch in the Nogo-A-specific region (NiG-Δ20) is strongly inhibitory for neurite outgrowth and cell spreading in vitro (Oertle et al., 2003d). In addition, the loop region between the two C-terminal hydrophobic domains of the RHD (called Nogo-66) has been shown to induce collapse of neuronal growth cones in vitro (GrandPré et al., 2000).

The RTN proteins are evolutionary conserved in eukaryotes (Oertle et al., 2003b), and therefore Nogo-A homologs may exist and impair CNS axon regeneration in amphibians. In frogs, CNS axons fail to regenerate in the spinal cord after metamorphosis (Beattie et al., 1990; Forehand and Farel, 1982). The inability of regeneration correlates with the nonpermissive properties of spinal cord myelin and oligodendrocytes in cocultures with axons, indicating the expression of inhibitory proteins in this region (Lang and Stuermer, 1996; Lang et al., 1995). CNS myelin and oligodendrocytes from the optic nerve and tectum, where amphibian axons do regenerate, were not inhibitory to growing axons in vitro (Lang et al., 1995). Reasons may lie in regional differences concerning

☆ Supplementary data associated with this article can be found, in the online version, at doi:10.1016/j.mcn.2003.09.021.

* Corresponding author. Fax: +49-7531-88 3894.
E-mail address: Claudia.Stuermer@uni-konstanz.de (C.A.O. Stuermer).

[1] Both authors contributed equally.

Available online on ScienceDirect (www.sciencedirect.com.)

1044-7431/$ - see front matter © 2003 Elsevier Inc. All rights reserved.
doi:10.1016/j.mcn.2003.09.021

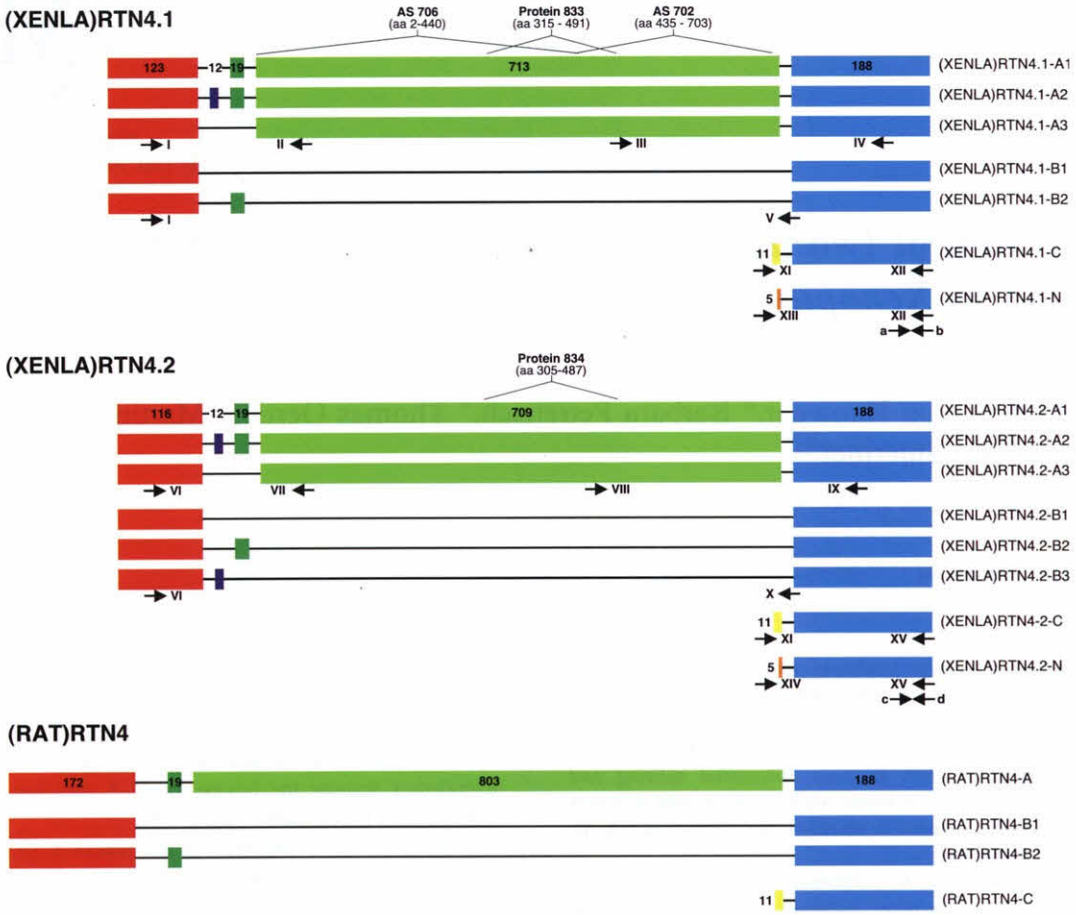

Fig. 1. Schematic representation of *Xenopus* nogo/rtn4 in comparison to rat nogo/rtn4 transcripts. Two *nogo/rtn4* genes were identified in *X. laevis* and the different transcripts were named according to the nomenclature guidelines for reticulon genes ((XENLA)rtn4.1, (XENLA)rtn4.2; see Experimental methods). Their overall structures correspond to mammalian rtn4. Nogo-A/rtn4-A consists of an N-terminal A/B-specific region (red), a central A-specific region (light green) and the RHD (blue). In the B-isoforms, the A-specific region is missing. For both the A- and B-isoforms, multiple minor splice variants exist due to the alternative usage of two (*Xenopus*) or one (mammals) small exons (dark blue and dark green). RTN4-C (yellow) and RTN4-N (orange) are transcribed from alternative promoters, but the RHD is the same as for the -A and -B isoforms. The amino acid length of the respective regions is depicted by Arabic numerals. Localizations of primers are indicated by arrows and Roman numerals (RT-PCR) or lower case letters (genomic PCR). The range of recombinant proteins used for the generation of polyclonal antisera against Nogo-A is outlined with brackets. AS, polyclonal antiserum.

the expression of myelin inhibitors or their subcellular localization, for example, surface exposure in myelin membranes or retention in the ER.

We used conserved sequence motifs of mammalian *nogo*-A to search for *Xenopus nogo/rtn4* homologs. Various transcripts corresponding to the three major isoforms rtn4-A, -B and -C were

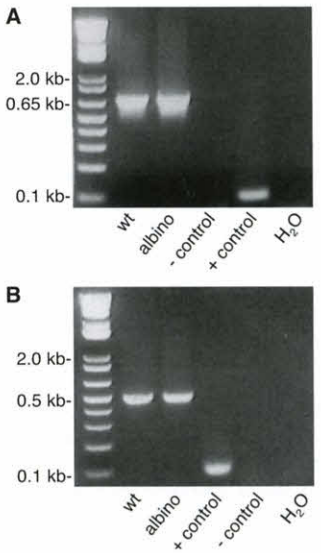

Fig. 2. PCR analysis of *Xenopus* rtn4 introns. The existence of two independent *nogo/rtn4* genes was proven by PCR analysis of intron sizes. Specificity of the used primer pairs for one of the two *rtn4* genes (primers a + b for rtn4.1 and primers c + d for rtn4.2; see Fig. 1) was verified by PCR on cloned plasmid DNA (+control; −control). (A) Primers a + b amplified the expected PCR product of 110 bp only on *rtn4.1* (lane 4) but not on *rtn4.2* (lane 3) plasmid DNA. On two different genomic DNA templates (prepared from either wild-type or albino *X. laevis*), the amplicon was 678 bp (lanes 1 and 2). (B) Primers c + d were specific for rtn4.2 (lane 3) and no amplification was achieved on rtn4.1-negative control plasmid (lane 4). The PCR product on genomic DNA templates was 490 bp (lanes 1 and 2). wt, wild-type.

identified. In contrast to mammals, we found an additional short, so far unknown, isoform termed rtn4-N. The *nogo/rtn4* gene underwent a *Xenopus* specific duplication, which would allow independent transcriptional regulation of the two *nogo* gene copies. Tissue-specific transcription of the different nogo/rtn4 cDNAs was analysed by RT-PCR. Nogo-A/RTN4-A protein expression was detected with *Xenopus* Nogo-A/RTN4-A specific antibodies in oligodendrocytes and major myelinated fiber tracts. Its distribution is comparable to the Nogo-A expression in mammals and—because Nogo-A forms are not found in zebrafish (Klinger et al., 2002; Oertle et al., 2003b)—indicates that the evolution of this neurite growth inhibitor has occurred in land vertebrates.

Results

Identification and characterization of Xenopus laevis rtn4

We have cloned full-length cDNAs of altogether 15 different *X. laevis* (XENLA) nogo/rtn4 transcripts by degenerate PCR, RACE and RT-PCR. Fig. 1 gives a schematic overview of these transcripts and illustrates the relationship between *Xenopus* and rat rtn4 isoforms. Based on RHDs, which form the C-terminal part of all RTN4 proteins, we were able to assign the sequences to two groups (rtn4.1, rtn4.2), indicating a *X. laevis*-specific gene duplication (see below). As in human, rat and mouse (Chen et al., 2000; GrandPré et al., 2000; Prinjha et al., 2000), the three major transcripts rtn4-A, -B and -C also exist for both *Xenopus* genes. Small, alternatively spliced exons lead to multiple mRNA variants of the -A and -B isoforms (Figs. 1 and 3). Unexpectedly, we identified an additional, so far unknown, rtn-4 isoform with a short N-terminus of 5 aa, which we named (XENLA)rtn4-N.

The full-length (XENLA)rtn4.1-A1/4.2-A1 sequences consist of 4024/3898 base pairs (bp), with open reading frames (ORFs) coding for 1043/1032 aa, respectively. Compared to rat Nogo-A, the coding regions are 120/131 aa shorter based on length differences both in the Nogo-A/B-specific regions (49/56 aa shorter) and the Nogo-A-specific regions (71/75 aa shorter). The RHDs are exactly as long as in the rat (188 aa; Fig. 1). At their C-termini, a dilysine ER retention motif (KRKAE) is present. *Xenopus* rtn4.1-A and rtn4.2-A each have one major (rtn4-A1) and two minor splice variants arising from the alternative usage of two small exons of 36 bp (12 aa) and 57 bp (19 aa; Fig. 1). These exons are either both present (rtn4-A2), both absent (rtn4-A3) or individually used (rtn4-A1). The 36-bp exon is unique for the *Xenopus rtn4* genes and was not identified in mammals (Oertle et al., 2003a). The full-length Nogo-A1/RTN4-A1 proteins and the respective rat ortholog share an overall identity of 34%, with the highest sequence conservation in the RHD. *Xenopus* RTN4.1-A1 and RTN4.2-A1 are 78.3% identical and are therefore more closely related to each other than to any other mammalian Nogo-A/RTN4-A. Rtn4.1-B and rtn4.2-B are alternative splice forms of rtn4.1-A and rtn4.2-A, respectively, sharing the respective N-terminal A/B-specific regions with the start codons, the RHDs and the untranslated regions (UTRs), but lacking the A-specific central exons (Fig. 1). The sequences surrounding the putative start methionines of rtn4.1-A/B and rtn4.2-A/B (cccGcc*ATG*G/gccGca*ATG*G) comply with the consensus motif for initiation of translation (gccAcc*ATG*G) that particularly requires a G residue following the ATG and a purine at position -3 (Kozak, 1996). Although there are no upstream stop codons in the cloned 5′ UTRs (110/118 bp), the consensus motifs

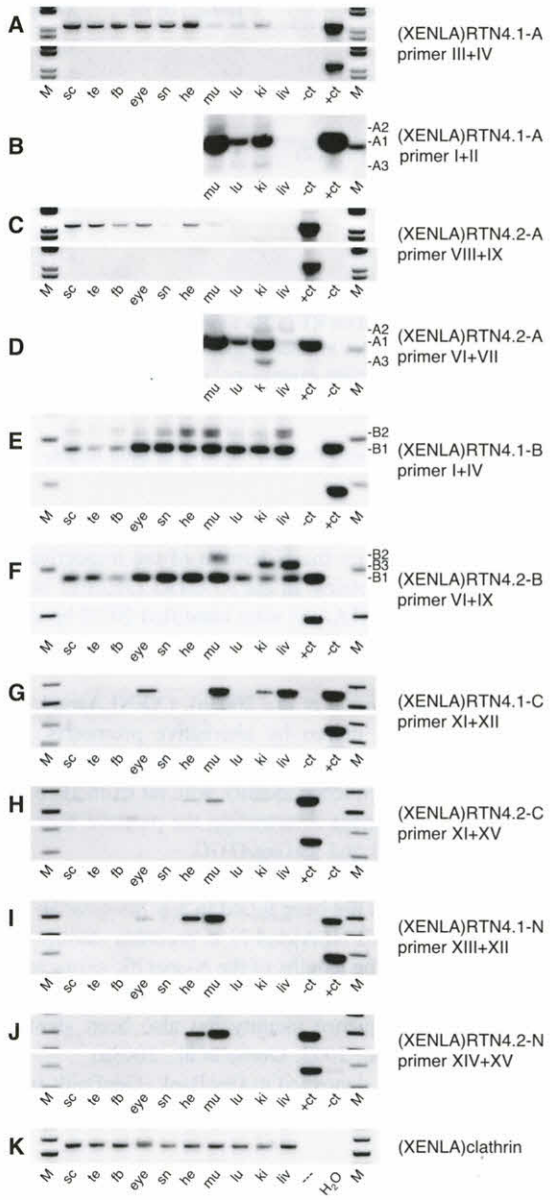

Fig. 3. RT-PCR analysis of *Xenopus* rtn4 mRNA expression. Transcripts of rtn4-A, -B, -C and -N were detected in various *Xenopus* tissues (upper row of panels A–J). Lanes +ct and −ct are control PCRs on plasmid DNAs to prove specificity of the primers for rtn4.1 and rtn4.2, respectively. A 'zero reverse transcriptase' negative control was conducted with each primer pair to show that no bands were amplified due to genomic DNA contamination of the templates (lower row of panels A–J). (A) Amplification of rtn4.1-A. (B) Detection of rtn4.1-A splice variants in nonneuronal tissues. (C) Amplification of rtn4.2-A. (D) Detection of rtn4.2-A splice variants in nonneuronal tissues. (E) Analysis of rtn4.1-B splice variants. (F) Analysis of rtn4.2-B splice variants. (G) Amplification of rtn4.1-C. (H) Amplification of rtn4.2-C. (I) Expression of rtn4.1-N. (J) Expression of rtn4.2-N. (K) RT-PCR with clathrin-specific primers served as positive control to ensure that equal amounts of cDNA template were used in each reaction. H_2O was a 'no template' control. sc, spinal cord; te, tectum opticum; fb, forebrain; sn, sciatic nerve; he, heart; mu, muscle; lu, lung; ki, kidney; liv, liver; +ct, positive control; −ct, negative control.

Table 1
Comparison of semiquantitative expression levels of the major RTN4 isoforms in *Xenopus* and mammals (human, rat)

	RTN4-A1		RTN4-B1		RTN-C		RTN4-N
	Xenopus	Human or rat	*Xenopus*	Human or rat	*Xenopus*	Human or rat	*Xenopus*
Spinal cord	++	++	+	+	–	±	–
Tectum[a]	++	++	+	+	–	±	–
Forebrain	++	++	+	+	–	±	–
Eye	++	++	++	+	+(4.1) – (4.2)	+	+(4.1) – (4.2)
Sciatic Nerve	++(4.1) + (4.2)	±	++	++	–	–	–
Heart	++	+	++	+	–(4.1) + (4.2)	–, +[b]	++
Muscle	±	+, –[c]	++	+	++(4.1) + (4.2)	++	++
Lung	±	–	++(4.1) + (4.2)	++	–	–	–
Kidney	±	–	++(4.1) + (4.2)	+	+(4.1) – (4.2)	+	–
Liver	–	–	++(4.1) + (4.2)	–	++(4.1) – (4.2)	+, –[b]	–

Data for *Xenopus* are based on RT-PCRs shown in Fig. 3 and Western blots (Fig. 4B) and apply to both genes if not indicated in parentheses. Data for human and rat are taken from tables in (Oertle and Schwab, 2003; Hunt et al., 2002a).
++, Strong expression; +, clear expression; ±, weak expression; –, no detectable expression.
[a] Tectum opticum in *Xenopus*; thalamus, amygdala, habenular nuclei in mammals.
[b] Conflicting data.
[c] Positive in immature skeletal muscle, negative in adult muscle.

and the absence of alternative start codons suggest that the identified methionines are the N termini of the respective (XENLA)RTN4-A and -B proteins. In the 3′ UTRs (782/681 bp), polyadenylation signals (AATAAA) were identified 20/27 bp upstream of the poly-A tails, proving that the entire 3′ -UTRs were cloned for both *rtn4* genes.

As in mammals (Oertle et al., 2003a), (XENLA)rtn4.1-C and (XENLA)rtn4.2-C are driven by alternative promoters. The C-specific exons each code for 11 aa that are 91% identical to each other and share 36% sequence identity with rat exon 1C (Oertle et al., 2003a). The sequences surrounding the putative start methionines are tcaGaa*ATG*G and tcaGag*ATG*G.

Interestingly, we identified a further isoform, rtn4-N, for both *Xenopus* genes that has not been found in any mammalian species. The transcription of (XENLA)rtn4-N is probably driven from an alternative promoter. The lengths of the N-specific exons are 16 bp (5 aa) and the encoded aa are 100% identical. An orthologous isoform with 80% sequence identity has also been identified in zebrafish (Klinger et al., 2002; Oertle et al., 2003b).

All sequences were deposited in GenBank (GenBank accession numbers, AY316183–AY316197).

Existence of two Xenopus rtn4 genes

Two *Xenopus* rtn4-A clones with a sequence divergence of 13% at the cDNA level were initially identified by PCR with degenerate primers (for details see Experimental methods). To test whether these two forms are alleles or independent *Xenopus rtn4* genes, the length and sequence identity of RHD introns were analysed (Fig. 2). Because rtn4-A, -B, -C and -N are isoforms transcribed from the same gene and share the RHD, evidence for two RHDs is sufficient to prove the existence of two independent *rtn4* genes. Based on the known intron/exon structure of the human and mouse orthologs (Oertle et al., 2003a), PCR was performed on genomic DNA to amplify intron IV sequences (between the 4th and 5th exon of the RHD; for primer sequences and positions, see Supplementary Table 1B and Fig. 1). Rtn4.l-specific primers amplified the expected product of 110 bp on rtn4.l-positive control plasmid DNA but not on rtn4.2 (negative control). PCR on two different genomic DNA templates (wild-type (wt) and albino) resulted in an amplicon of 678 bp (Fig. 2A). In contrast, rtn4.2-specific primers amplified the expected product on rtn4.2-positive control plasmid DNA, but not on an rtn4.1-negative control. On genomic DNA, the amplicon was 490 bp (Fig. 2B). Thus, this intron of *rtn4.1* is 188 bp longer. Its sequence differs by 36% from

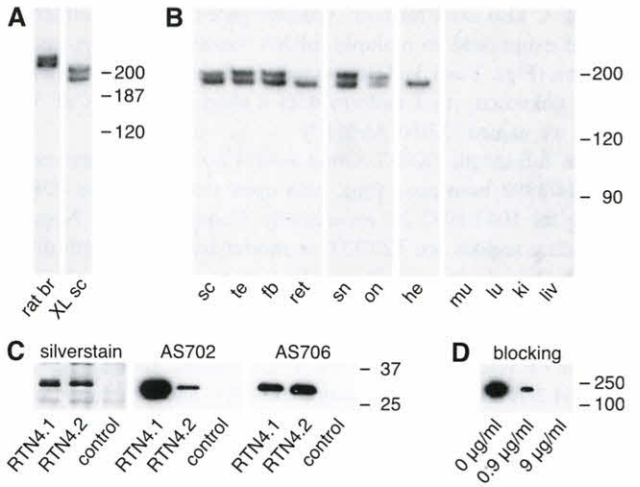

Fig. 4. Western blot analysis of *Xenopus* Nogo-A/RTN4-A protein expression. (A) *Xenopus* Nogo-A/RTN4-A proteins detected with AS702 in the spinal cord homogenate (XL sc) exhibit a lower molecular weight than the homologous rat protein detected with AS472 (Chen et al., 2000) in the brain homogenate (rat br). Rat and *Xenopus* Nogo-A proteins migrate aberrantly slow in SDS-PAGE due to their acidic nature. (B) Expression of Nogo-A/RTN4-A proteins in different *Xenopus* tissues was analysed with the Nogo-A specific AS702. sc, spinal cord; te, tectum opticum; fb, forebrain; ret, retina; sn, sciatic nerve; on, optic nerve; he, heart; mu, muscle; lu, lung; ki, kidney; liv, liver. (C) A part of RTN4.1-A (protein 833, see Fig. 1), RTN4.2-A (protein 834) and an unrelated control protein were recombinantly expressed (left panel, silver staining) and Western blots were probed with AS702 (middle panel) and AS706 (right panel). AS702 as well as AS706 recognized both RTN4.1-A and RTN4.2-A. (D) Tectum opticum homogenate was probed with AS706 and a concentration-dependent signal reduction was achieved by blocking the antiserum with increasing amounts of recombinantly expressed 706 protein (0, 0.9, 9 µg/ml). AS, polyclonal antiserum.

its *rtn4.2* counterpart. Similar results were obtained by the analysis of other introns and of the 3′ UTRs (data not shown), proving the existence of two independent *rtn4* genes in *X. laevis*.

Whether the two *rtn4* genes result from the *X. laevis* specific tetraploidization was evaluated by computing the rates of synonymous (silent) and nonsynonymous (aa altering) nucleotide substitutions (d_S and d_N; Supplementary Table 2). Assuming that silent mutations accumulate at approximately constant rates, the elapsed time since the duplication is proportional to d_S of the two *Xenopus* rtn4-A transcripts and can be calculated by comparison to the corresponding rates of the human and rat cDNAs (Hughes and Hughes, 1993). Consistent with an *rtn4* gene duplication more recent than the divergence of rodents and primates approximately 80–100 million years ago (MYA) (Li et al., 1990), d_S of the two *Xenopus* rtn4-A transcripts (26.6 ± 2.2 substitutions/100 sites) was lower than the mammalian d_S (44.3 ± 3 substitutions/100 sites). This rate is comparable to d_S of other duplicated *Xenopus* genes (Hughes and Hughes, 1993), suggesting that the *rtn4* gene duplication occurred during the tetraploidization event approximately 30 MYA. Unexpectedly, the rate of aa altering mutations (d_N) of the rtn4-A transcripts (10.3 ± 0.7 substitutions/100 sites) was explicitly higher than for other duplicated *Xenopus* genes, almost reaching the d_N of the rat and human rtn4 orthologs (11.9 ± 0.7 substitutions/100 sites). However, neither of the two copies evolved significantly faster than the other at nonsynonymous sites (59.6 ± 2.5 compared to 58.4 ± 2.6), as was shown by separate comparison of each *Xenopus* gene to the human rtn4 ortholog.

This result indicates that both *Xenopus rtn4* genes evolved equally fast and that neither gene copy is redundant and therefore free to accumulate mutations without constraint.

RT-PCR analysis of Xenopus rtn4 mRNA expression

Transcription of *rtn4* in different tissues of adult *X. laevis* was analysed by RT-PCR (for an overview see Table 1). Using primers that do not discriminate among the three different rtn4.1-A splice variants (primers III + IV, see Fig. 1), expression was predominantly observed in CNS tissues, that is, spinal cord, tectum opticum, forebrain and eye, but also in sciatic nerve and heart (Fig. 3A). Faint bands indicating low expression levels were visible in the muscle, lung and kidney. Rtn4.2-A transcripts, in comparison, were expressed in a similar pattern at an overall lower level, especially in sciatic nerve, and under these PCR conditions not detectable in the lung, kidney and liver (Fig. 3C, primers VIII + IX). To distinguish among the three splice products of rtn4-A (-A1, -A2 and -A3), we applied sensitive RT-PCR (see Experimental methods). Amplification of the region that could vary in length due to the alternative usage of the two 36 and 57 bp exons (primer I + II for rtn4.1-A and VI + VII for rtn4.2-A; Fig. 1) detected only the major splice variant (-A1; with the 57 bp exon and without the 36 bp exon) in all neuronal tissues and heart (data not shown). In nonneuronal tissues, additional, so far undetected expression and alternative splice products were revealed. For rtn4.1, the major transcript (-A1) was expressed in the muscle, lung and kidney, whereas rtn4.1-A2 (containing both exons) was present only in muscle and rtn4.1-A3 (both exons missing) only in kidney (Fig. 3B). Using this more sensitive PCR for rtn4.2, we unexpectedly found -A1 mRNA transcripts in all nonneuronal tissues (Fig. 3D). Rtn4.2-A2 was detectable in the kidney and liver while rtn4.2-A3 expression was restricted to the kidney.

Transcripts for both rtn4-B1 forms (the main −B splice variant) were verified in all tissues analysed (Figs. 3E and F), although expression levels were low in the spinal cord, tectum opticum, forebrain (rtn4.1 and -2) and lung (rtn4.2). Hence, transcription of the rtn4-B forms predominantly in nonneuronal tissues is almost complementary to the rtn4-A expression. For rtn4.1-B, one additional splice form appeared in all tissues (rtn4.1-B2; Fig. 3E). In contrast, tissue-specific alternative splicing was observed for rtn4.2, with rtn4.2-B2 occurring only in the muscle and rtn4.2-B3 in the kidney and liver (Fig. 3F).

Rtn4.1-C mRNA was detectable in the eye, muscle, kidney and liver (Fig. 3G). In comparison, rtn4.2-C transcription occurred at a much lower level with clearly detectable expression only in the heart and muscle (Fig. 3H). Similarly, the rtn4.1-N and rtn4.2-N isoforms were both mainly expressed in the heart and muscle (Figs. 3I and J).

Taken together, these RT-PCR results indicate that the various transcripts of each *Xenopus rtn4* gene are differentially expressed. While the major -A, -B and -N isoforms have a comparable expression pattern for both *Xenopus rtn4* genes, the distribution of the -C form as well as of minor -A and -B splice variants differs between the two genes.

Distribution of Xenopus Nogo-A/RTN4-A protein

Selected A-specific regions of RTN4.1 were recombinantly expressed (see Experimental methods) and used for the generation of polyclonal antisera AS702 and AS706 (Fig. 1). To show whether the obtained antisera are specific for RTN4.1 or recognize both *Xenopus* RTN4-A proteins, a part of RTN4.1-A (protein 833, see Fig. 1), RTN4.2-A (protein 834) and an unrelated control protein were recombinantly expressed (Fig. 4C, left panel) and Western blots were probed with AS702 (Fig. 4C, middle panel) and AS706 (Fig. 4C, right panel). Both antisera recognized RTN4.1-A as well as RTN4.2-A proteins (Fig. 4C) and did not discriminate between the RTN4-A proteins of the two genes.

In *Xenopus* spinal cord homogenate, AS702 (Fig. 4A) and AS706 (data not shown) recognized two bands of approximately 200 kDa. Because the calculated molecular weights (113.99/113.59 kDa) and pIs (4.4/4.5) of the two Nogo-A1/RTN4-A1 proteins are almost identical, the second band most probably represents a different posttranslational modification of one or both proteins. In comparison to rat Nogo-A (about 220 kDa; Fig. 4A), the *Xenopus* proteins migrated faster in SDS-PAGE, which is consistent with the 13 kDa difference in the calculated molecular weights. Western blot studies on *Xenopus* tissues revealed that Nogo-A/RTN4-A expression was mainly restricted to the nervous system, which is in accordance with the RT-PCR analysis. In addition to spinal cord, two protein forms were detected in the tectum opticum, forebrain, sciatic and optic nerves, but only one was found in the retina and heart (Fig. 4B). No Nogo-A/RTN4-A protein was observed in nonneuronal tissues (i.e., muscle, lung, kidney or liver). Specificity of polyclonal AS706 for *Xenopus* RNT4-A was shown on Western blots of the tectum opticum homogenate. Concentration-dependent signal reduction was achieved by blocking the antiserum with increasing amounts of recombinantly expressed 706 protein (Fig. 4D). Adding 0.9 μg/ml 706 protein to the antibody solution significantly reduced the signal whereas a concentration of 9 μg/ml led to a complete loss.

Immunostaining on cross-sections of adult *Xenopus* spinal cord revealed Nogo-A/RTN4-A expression in myelinated tracts of the

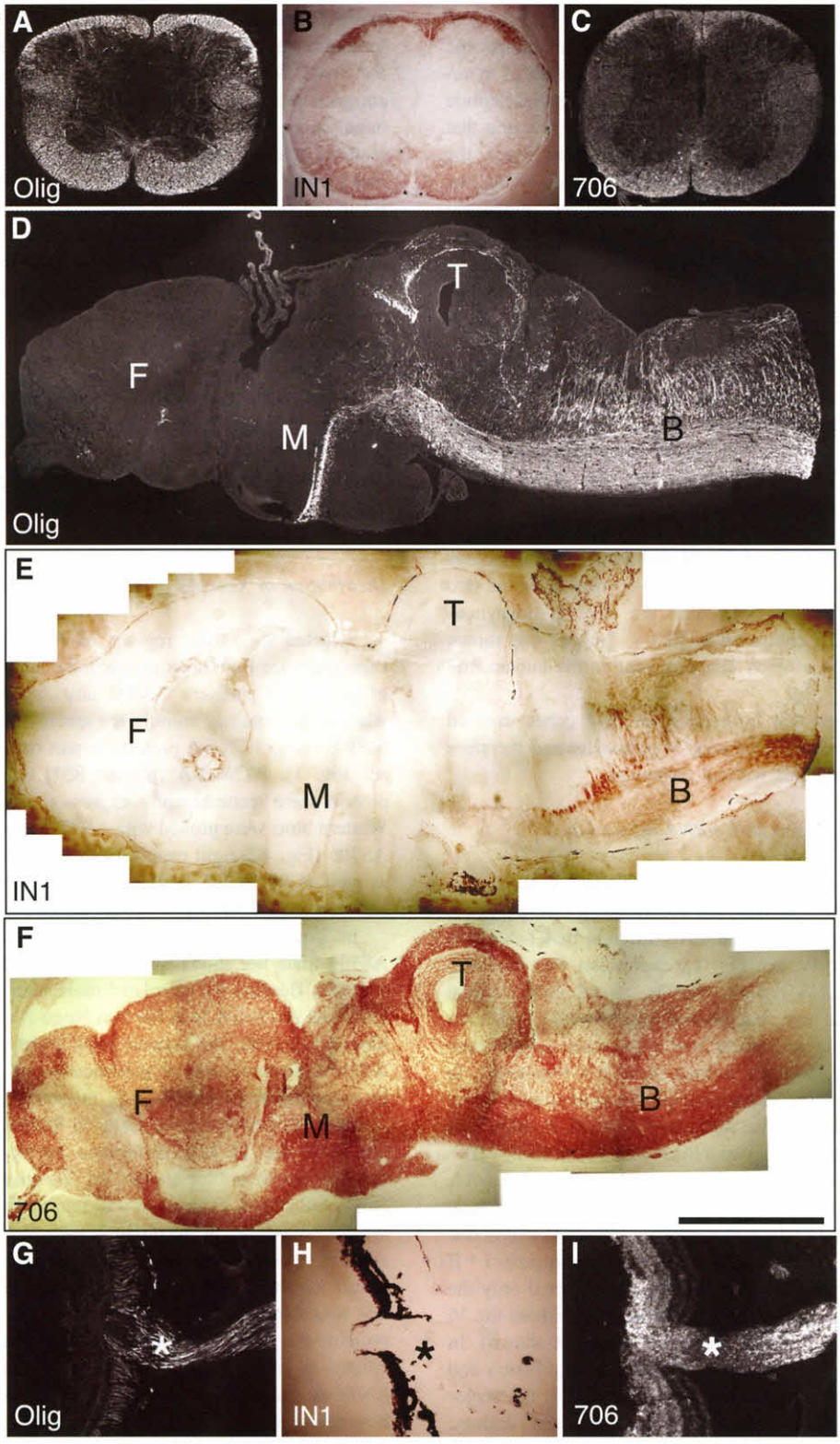

Fig. 5. Immunolocalisation of Nogo-A/RTN4-A protein in the *Xenopus* CNS. Sections of *Xenopus* spinal cord (A–C; cross), brain (D–F, sagittal) and optic nerve (G–I, longitudinal) were immunostained with AS706 (C, F, I). The expression of Nogo-A/RTN4-A protein was compared to the distribution of the oligodendrocyte-specific marker Olig (A, D, G) and the mAb IN-1 staining (B, E, H). Nogo-A is detected in myelinated fiber tracts of the spinal cord (C), brain (F) and optic nerve (I). AS706 also labels unmyelinated regions in the forebrain or midbrain (F). B, brainstem; F, forebrain; M, midbrain; T, tectum opticum; *, optic nerve. The staining of photoreceptors (G) is unspecific. Scale bar is 500 μm in A–C, 1000 μm in D–F and 200 μm in G–I.

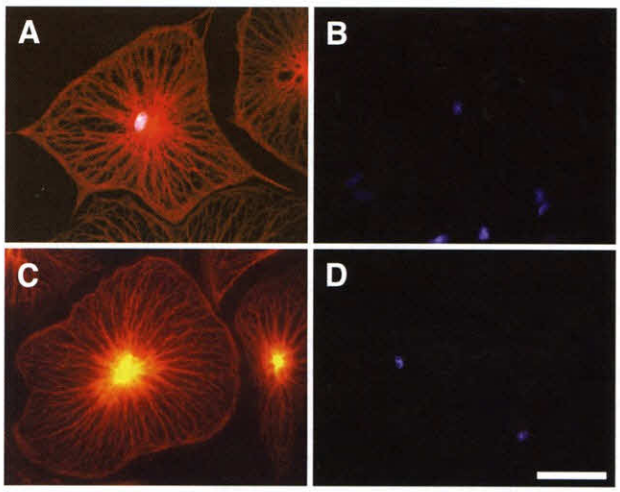

Fig. 6. Detection of Nogo-A/RTN4-A protein in *Xenopus* oligodendrocytes. Cultured oligodendrocytes isolated from *Xenopus* spinal cord (A, B) or optic tectum (C, D) were stained with the Nogo-A/RTN4-A specific AS706 (red) and the nuclear stain DAPI (blue). Nogo-A/RTN4-A is predominantly detected in intracellular compartments after permeabilisation (A, C). This staining is blocked by preincubation of AS706 with the protein used for antibody generation (B, D). Scale bar is 50 μm.

white matter (Fig. 5C), as was observed for the rat Nogo-A protein (Chen et al., 2000). The staining pattern was comparable to the distribution of the oligodendrocyte markers Olig (Fig. 5A), O4 (data not shown) and of the IN-1 antibody (Fig. 5B). On sagittal sections of *Xenopus* brain, Olig labeled myelinated longitudinal and transverse fiber tracts in the ventral part of the brainstem (Fig. 5D). Corresponding fiber tracts were also detected, though weaker, with the IN-1 antibody (Fig. 5E). In addition, Olig brightly stained a single layer in the optic tectum that was not revealed with IN-1. Nogo-A/RTN4-A expression detected after Clark's fixation with AS706 (Fig. 5F) and AS702 (data not shown) encompassed myelinated as well as cellular regions of the *Xenopus* brain. Myelinated fiber tracts in the brainstem and in the optic tectum were stained. In addition, extensive labeling of nonmyelinated areas that has also been demonstrated for rat Nogo-A (Huber et al., 2002) was observed especially in the forebrain region (Fig. 5F).

Myelin in the adult optic nerve was detected with the Olig marker (Fig. 5G) and corresponded to staining pattern of AS706 (Fig. 5I) and AS702 (data not shown), indicating Nogo-A/RTN4-A expression in the optic nerve and tract. The IN-1 antibody, however, failed to label the *Xenopus* optic nerve (Fig. 5H), which is consistent with our earlier results (Lang et al., 1995).

Localization of Nogo-A/RTN4-A protein in *Xenopus* CNS myelin was consolidated by immunostaining of cultured oligoden-

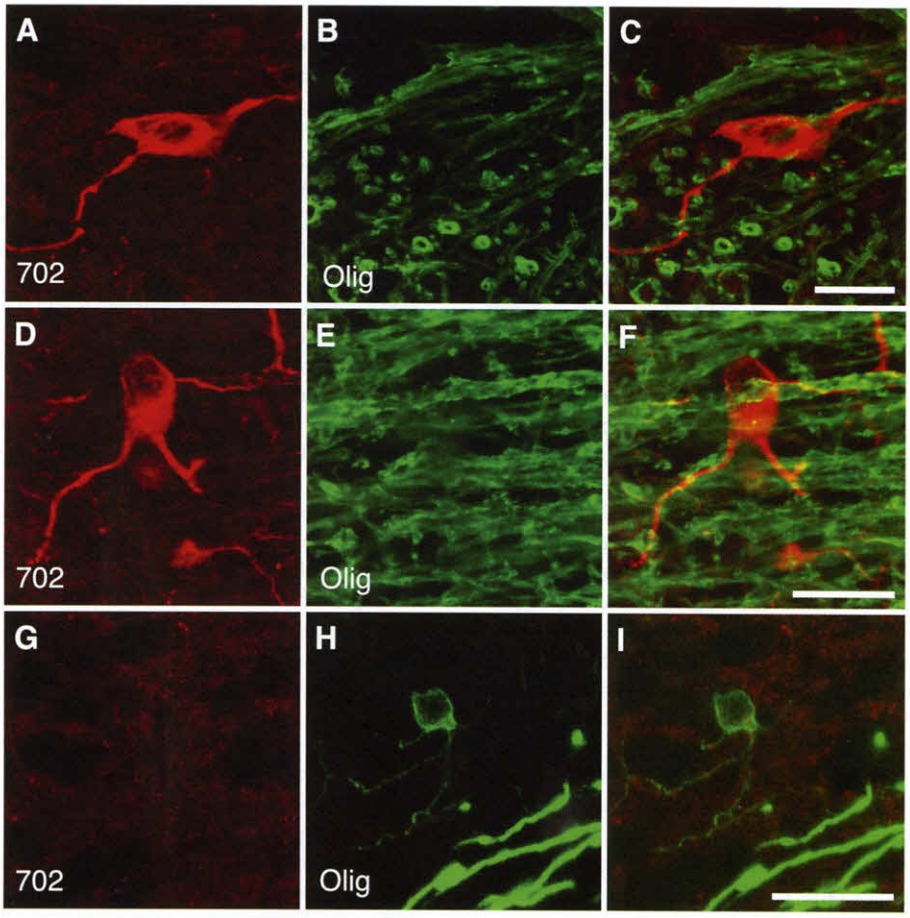

Fig. 7. Detection of Nogo-A/RTN4-A protein in neurons. Confocal microscopic analysis was performed on PFA-fixed sections of *Xenopus* spinal cord (A–C) and brain (D–I). The cellular staining observed with AS702 (A, D) does not colocalise with the myelin marker Olig (B, E), indicating neuronal expression of Nogo-A/RTN4-A. With this fixation protocol, no staining of oligodendrocyte cell bodies (identified by Olig; H) was observed with AS702 (G). Superpositions of the two stainings are shown in C, F and I, respectively. Scale bar is 20 μm.

drocytes isolated from the spinal cord (Fig. 6A) and optic tectum (Fig. 6C), respectively. After permeabilisation, oligodendrocytes from both tissues were strongly positive for Nogo-A/RTN4-A—in particular, the radially organised cytoplasm (Figs. 6A and C). Antibody specificity for *Xenopus* Nogo-A/RTN4-A was verified in control experiments. AS706 no longer stained oligodendrocytes from the spinal cord (Fig. 6B) and tectum opticum (Fig. 6D) after preincubation with the recombinant protein used for its generation.

The staining pattern with *Xenopus* Nogo-A/RTN4-A antisera was strongly dependent on the fixation method. After formaldehyde fixation, Nogo-A/RTN4-A was detected in specific cells and their processes in the spinal cord (Fig. 7A) and brain sections (Fig. 7D). These cells were not recognized by the oligodendrocyte marker Olig (Figs. 7B and E and superpositions in Figs. 7C and F) and probably represent neurons, as shown in the rat (Huber et al., 2002). Under these conditions, Nogo-A/RTN4-A staining of white matter and oligodendrocyte cell bodies (identified by Olig, Fig. 7H) was lost (Fig. 7G).

These results demonstrate that *Xenopus* Nogo-A/RTN4-A proteins are expressed in oligodendrocytes, CNS myelin and subpopulations of neurons. This pattern is comparable to that of the rat ortholog, which may indicate related functions.

Discussion

Here, we report the identification of *nogo/rtn4* genes in *X. laevis* and provide evidence for the expression of Nogo-A homologous proteins. Inhibitory proteins like Nogo-A, MAG and OMgp (Chen et al., 2000; McKerracher et al., 1994; Wang et al., 2002a) are suggested to impair axonal regeneration in the adult mammalian CNS. Because *Xenopus* spinal cord oligodendrocytes and CNS myelin also exert inhibitory functions in vitro (Lang et al., 1995), similar proteins are expected in this species. In contrast, CNS axons readily regenerate in the optic nerve and spinal cord of fish and urodeles (Clarke et al., 1988; Gaze, 1970). Anura, like *X. laevis*, take an intermediate position: retinal ganglion cell axons are capable of lifelong regeneration (Gaze, 1970) but spinal cord fiber tracts fail to regenerate after metamorphosis and myelination of axons (Beattie et al., 1990). Our present results show that Nogo-A orthologs as candidate growth inhibitory factors exist in frogs.

We identified two independent *rtn4* genes (*rtn4.1* and *rtn4.2*) that result from the tetraploidization of the *Xenopus* genome. As in mammals, several mRNA transcripts are generated from *rtn4.1* and *rtn4.2* either through alternative splicing (rtn4-A; rtn4-B) or probably alternative promoter usage (rtn4-C; rtn4-N). The sequences of *Xenopus* rtn4-A, -B and -C are related to the three major transcripts of the mammalian *nogo/rtn4* gene whereas *Xenopus* rtn4-N is a newly identified short form that has not been identified in mammals (Oertle et al., 2003a).

The expression of the main *Xenopus* Nogo-A/RTN4-A isoforms (RTN4-A1) of both *rtn4.1* and *rtn4.2* genes is mostly restricted to CNS regions and to the heart as shown by RT-PCR and Western blotting. This pattern is comparable to Nogo-A expression in mammals as summarised in Table 1. Immunostainings with antisera raised against *Xenopus* Nogo-A/RTN4-A on tissue sections are also consistent with the Nogo-A distribution in rodents (Huber et al., 2002; Josephson et al., 2001; Wang et al., 2002b). *Xenopus* Nogo-A/RTN4-A is expressed in myelinated tracts of the spinal cord and hindbrain, that is, regions labeled by the myelin marker Olig (Steen et al., 1989). This distribution corresponds to the outcome of earlier functional assays demonstrating the presence of axon growth inhibitory activity in myelin and oligodendrocytes of the *Xenopus* spinal cord (Lang et al., 1995). *Xenopus* Nogo-A/RTN4-A specific antisera also labeled isolated oligodendrocytes in culture. Thus, the distribution of *Xenopus* Nogo-A/RTN4-A in oligodendrocytes and CNS myelin is consistent with its postulated role as an inhibitor of axon regeneration.

However, Nogo-A/RTN4-A1 is also detected in myelin and oligodendrocytes of the optic nerve and the forebrain. Moreover, RTN4-A1 proteins are already expressed early in development (data not shown) when oligodendrocytes or neurons are not yet present. An early presence of Nogo-A has also been described in a variety of foetal rat tissues (Huber et al., 2002; Josephson et al., 2001). This early appearance and the intracellular localization of Nogo-A/RTN4-A suggest further, yet unidentified, functions that are not related to axonal growth inhibition.

The expression pattern revealed by RTN4-A-specific antisera differs from the weak and more restricted staining observed with mAb IN-1. One speculation is that IN-1 recognizes a Nogo-A modification or conformational epitope relevant for surface exposure and function. This would explain why only mAb IN-1 is able to discriminate between spinal cord and forebrain oligodendrocytes and to partially neutralize the inhibitory activity of *Xenopus* spinal cord and hindbrain myelin (Lang et al., 1995). This implies that changes in subcellular distribution (intracellular vs. surface) or posttranslational modifications are essential for the acquisition of the suggested inhibitory activity of Nogo-A in the adult CNS in vivo (Oertle et al., 2003d). Future analyses of the inhibition process and the elucidation of the respective roles of *Xenopus* RTN4.1-A and RTN4.2-A will be required to address those unresolved problems. Moreover, relevant axonal receptors remain to be identified. The contribution of other inhibitory myelin components such as MAG, OMgp and proteoglycans (Morgenstern et al., 2002) needs to be considered and the potential role of Nogo-66 in the regeneration or inhibition scenario (GrandPré et al., 2000) has to be clarified in frogs.

Apart from myelinated regions, *Xenopus* Nogo-A/RTN4-A antisera stain forebrain and midbrain regions that are not detected by myelin markers. These are seemingly neurons and neuropil, which is consistent with the detection of mammalian Nogo-A in neurons and neuronal processes (Huber et al., 2002; Josephson et al., 2001; Wang et al., 2002b). The putative neuron-specific functions of Nogo-A, which probably differ from the oligodendrocyte-related inhibitory activity, remain to be explored.

Compared to the preferential expression of Nogo-A/RTN4-A in the nervous system, the -B isoforms are ubiquitously expressed with highest levels in nonneuronal tissues (Table 1). High-level expression of the Nogo-A splice form in a specific tissue seems to be paralleled by low levels of the -B isoforms, as is observed in mammals (Oertle et al., 2003a). Besides the many similarities between *Xenopus* and mammalian Nogo-A expression, differences exist. The -A isoform is not detected in mammalian lung and kidney, but is present in these organs in *Xenopus*, and Nogo-B in liver is only found in *Xenopus* (Table 1; Hunt et al., 2002b; Oertle and Schwab, 2003). In addition, more minor splice variants of Nogo-A and -B exist in *Xenopus* than in mammals, resulting from the alternative usage of two small exons located between the A/B-specific exon and the large A-specific exon (Fig. 1). The weak expression of these minor splice variants is comparable to the expression levels of the

mammalian minor splice variants (rtn4-B2, -D, -E, -F, -G, -Aa, -Ab; Oertle et al., 2003a) and could indicate a modulatory or developmentally regulated role as suggested for the human testis-specific RTN4-E splice variant (Zhou et al., 2002).

As in mammals, *Xenopus* RTN4-C is enriched in the adult skeletal muscle (Table 1). The *Xenopus* rtn4.1-C isoform is also expressed in the liver, eye and kidney. In contrast, the rtn4.2-C paralog is hardly detectable except for the muscle. This could indicate that the putative *Xenopus rtn*4.2-C promoter is undergoing transcriptional silencing.

The rtn4-N mRNAs have a similarly restricted expression pattern, both being enriched in the heart and muscle (Fig. 3; Table 1). An N-specific exon has not been identified in mammals. In zebrafish, however, a homologous rtn4-N is present, but no rtn4-A, -B and -C transcripts (Klinger et al., 2002). It can therefore be hypothesized that the N-terminal sequences specific for rtn4-A/-B and rtn4-C were newly acquired during the evolution of land vertebrates (Oertle et al., 2003b). Accordingly, amphibians (e.g., *X. laevis*) express the 'ancestral' rtn4-N (that is also found in fish) and the 'modern' rtn4-A, -B and -C forms present in 'higher' vertebrates. *Xenopus* is, so far, the evolutionary 'lowest' organism that has the exceptionally large Nogo-A-specific exon, which codes for the potent inhibitory region NiG-Δ20 contained only in Nogo-A (Oertle et al., 2003d). Hence, the *Xenopus rtn4* genes might help to elucidate how Nogo-A acquired its inhibitory function. Conversely, *Xenopus* expresses the 'ancient' isoform rtn4-N, allowing the exploration of 'old' rtn4 features that are relevant in fish and frogs.

The duplication of *Xenopus nogo/rtn*4 was dated to approximately 30 MYA using the rate of silent nucleotide substitutions as a "molecular clock" (Hughes and Hughes, 1993). In general, genome duplication events increase the amount of genetic material, which is considered as a prerequisite for the development of new genes with new functions. Duplicated genes can adopt different fates: both are expressed and have similar functions, one copy accumulates mutations and eventually turns into a nonfunctional pseudogene, or a series of nondeleterious aa-altering mutations transforms one copy into a gene with a new function, as can be determined by a significantly faster evolutionary rate (Van de Peer et al., 2001). On the other hand, mutations in regulatory elements together with the conservation of coding regions can alter the spatiotemporal expression of two genes with comparable function. The respective *Xenopus* rtn-4 transcripts of both genes display similar expression patterns, suggesting that the promotor regions responsible for the transcriptional regulation of these isoforms did not undergo major functional changes after the duplication event. Thus, these genes appear to be redundant rather than complementary, which is also supported by our observation that neither of the two copies in comparison to the human ortholog evolved faster. However, both *rtn4* genes accumulated more aa-altering mutations than one might expect for an evolutionary time of approximately 30 MYA (Hughes and Hughes, 1993), which suggests the commencement of a potential diversification and of functional changes of both copies.

The present identification of *nogo/rtn4* in *X. laevis* and the analysis of the expression pattern of Nogo-A/RTN4 provide the first step towards understanding the evolution of myelin-associated proteins with axonal growth-inhibiting effects. Future experiments will determine the contribution of Nogo-66 and the Nogo-A-specific region to the growth inhibitory properties of *Xenopus* spinal cord myelin. A possible approach to tackle this issue is the generation of function-blocking antibodies binding to the oligodendrocyte surface. In addition, this study is a first entry point for functional analysis of Nogo-A during development and axonal growth.

The synthesis of ancient and modern features within the *nogo/rtn4* gene locus of *Xenopus* as well as the indications for a beginning diversification of the duplicated paralogs is relevant for the comprehension of gene evolutionary processes, particularly in the transition to land vertebrates.

Experimental methods

Animals

All animals were kept at the animal research facility of the University of Konstanz in compliance with animal welfare legislation. *X. laevis* were anesthetized and killed in a 0.03% solution of MS222 (Sigma-Aldrich, Seelze, Germany) for tissue preparation. Chinchilla bastard rabbits were used for immunization and RTN4 antibody generation.

Nomenclature of Xenopus nogo/rtn4 transcripts

Xenopus nogo transcripts were named according to the nomenclature guidelines for reticulon genes (Oertle et al., 2003b). In brief, *rtn* serves as a gene symbol for chordate reticulons. Paralogous *rtn* sequences are arbitrarily numbered with *nogo* being *rtn4*. Reticulon genes that have been duplicated within the same species share the same symbol and differ by an additional number (e.g., *rtn4.1* and *rtn4.2*). To distinguish *rtn* genes of various species, a prefix according to the identification code proposed by SWISS-PROT is used (e.g., (XENLA)*rtn4.1*). Alternative transcripts from different promoters receive a new letter (e.g., (XENLA)rtn4.1-A, (XENLA)rtn4.1-C), while alternatively spliced transcripts derived from the same promoter have the same letter but are distinguished by the consecutive numbering (e.g., (XENLA)rtn4.1-A1, (XENLA)rtn4.1-A2). For historical reasons, rtn4-A and rtn4-B do not comply with this rule (Chen et al., 2000; GrandPré et al., 2000; Prinjha et al., 2000).

Cloning with degenerate primers

Total RNA was isolated from *X. laevis* embryos older than stage 50 (Trizol; Wak Chemie, Bad Homburg, Germany) and reverse-transcribed following the manufacturer' s instructions (Ready to Go T-primed first strand kit, Amersham Biosciences, Freiburg, Germany). Conserved sequence motifs of the nogo-A cDNA of rat, human and chicken were used to design degenerate primers (Nogo-A-RN/se1: 5′-CA[AG] GA[AG] AC[AGCT] GA[AG] GC[AGCT] CC[AGCT] TA[CT] AT-3′, Nogo-A-RN/as2: AC[AG] TA[AGCT] GT[AG] AA[AGCT] ACC CAC AT). Using standard PCR, two different partial cDNA clones (1.2 kb) coding for two *Xenopus rtn4* genes were amplified. Both clones contain nogo-A-specific sequences (837 bp for (XENLA)rtn4.1 and 849 bp for (XENLA)rtn4.2) and parts of the reticulon homology domain (381 and 384 bp, respectively).

5′- and 3′-rapid amplification of cDNA ends (RACE) and full-length cloning

The SMART RACE cDNA amplification kit (BD Clontech, Heidelberg, Germany) was used to determine the 5′ and 3′

sequences including the putative start methionines and 3′-non-coding regions for both the (XENLA)rtn4.1 and (XENLA)rtn4.2, transcripts. Total RNA (1.3 μg/reaction) served as template for the synthesis of first-strand 5′-Ready cDNA using 5′-CDS and SMART II oligonucleotides and 3′-Ready cDNA using 3′-CDS primer, according to the manufacturer' s protocol.

The rtn4-A specific primer 5′-RACE GSP XL (5′-AGA ATC TGG TGA GCT TTC ATC GGA GGG C-3′ ; bp 1797–1824 of (XENLA)rtn4.1-A3 and bp 1764–1791 of (XENLA)rtn4.2-A3, respectively) was used to amplify 5′-cDNA ends of both rtn4-A transcripts. To clone additional rtn4 isoforms (B, C and N), a 5′-RACE primer in the reticulon homology domain (RHD) was used (5′-RACE GSP XL 3: 5′-CTG GCA CCG CCA GGT TGG ACT CCA AGA TGG-3′ ; bp 2720–2749 of (XENLA)rtn4.1-A3 and bp 2687–2716 of (XENLA)rtn4.2-A3, respectively).

The 3′ ends including UTRs were completed using primer 3′ RACE GSP XL (5′- CCC CCT TCG AAG GAA GAT GAT GGT TCC-3′ ; bp 2422–2448 of (XENLA)rtn4.1-A3) and 3′ RACE GSP XL2 (5′- AAC CCG AAC CCC CTT CAA AGA AAG ATG AGG-3′ ; bp 2375–2404 of (XENLA)rtn4.2-A3), respectively. All RACE reactions were performed as described in the manufacturer's protocol, and PCR products were directly cloned into pCRII-TOPO vector (Invitrogen, Karlsruhe, Germany).

Full-length clones of the alternative nogo transcripts (rtn4-A, -B, -C and -N) were obtained for both *X. laevis nogo* genes using primers located at the 5′ and 3′ ends of the various transcripts. (XENLA)rtn4.1- and (XENLA)rtn4.2-specific dbESTs were identified as described elsewhere (Oertle et al., 2003b). Sequences were deposited in GenBank (GenBank accession numbers, AY316183–AY316197).

DNA sequencing and sequence analysis

Plasmid DNA of RACE and full-length clones was prepared using the QIAprep® 8 Miniprep Kit (Qiagen, Hilden, Germany). Both DNA strands were sequenced using the Abi Prism® BigDye™ Terminator Cycle Sequencing Kit (Applied Biosystems, Darmstadt, Germany). Sequencing products were analysed on an AbiPrism 3100 Genetic Analyser (Applied Biosystems). Single sequences were assembled using the Lasergene software package (GATC Biotech, Konstanz, Germany). Molecular evolutionary analyses were conducted using *MEGA* version 2.1 (Kumar et al., 2001). In brief, sequences were aligned at the amino acid level by the CLUSTALW program and gaps were pair-wise deleted. Numbers of synonymous nucleotide substitutions per synonymous site (d_S) and nonsynonymous substitutions per nonsynonymous site (d_N) were estimated (Nei and Gojobori, 1986) for both (XENLA)rtn4 sequences and the human ortholog.

RT-PCR

Various tissues (spinal cord, tectum opticum, forebrain, retina, sciatic nerve, heart, muscle, lung, kidney, liver) were dissected from adult *X. laevis* and used for preparation of total RNA with QIAshredders and the RNeasy Mini Prep Kit (Qiagen) following the manufacturer's instructions (<30 mg tissue/column). Muscle tissue was additionally subjected to proteinase K digestion (200 μg/30 mg tissue).

First-strand cDNA was synthesized with the Superscript First-Strand Synthesis System for RT-PCR (Invitrogen). Up to 5 μg of total RNA was reverse-transcribed under standard conditions with 0.5 μg oligo$(dT)_{12-18}$ primer. Zero transcriptions (without Superscript II in the reaction) were performed in parallel to control for genomic DNA contaminations in subsequent PCRs. Amount and quality of the different cDNA samples were evaluated comparing the expression level of the housekeeping gene clathrin (primers: 5′ -GAC AGT GCC ATC ATG AAT CC-3′ and 5′-TTT GTG CTT CTG GAG GAA AGA A-3′; 28 cycles, annealing 50 °C, elongation 60 s). Using this PCR as an internal reverence, the concentration of the cDNAs was adjusted to comparable levels.

A standard 25-μl PCR reaction contained 2.5 μl of 10× reaction buffer (500 mM NaCl/15 mM $MgCl_2$/100 mM Tris–Cl, pH 9.0; Amersham Biosciences), 0.3 μl dNTP mix (10 mM each), 1 μl of first strand cDNA, 0.75 U Taq DNA polymerase (Amersham Biosciences) and 50 pmol of the appropriate sense and antisense primers (see Supplementary Table 1A for sequence information and arrows in Fig. 1 for primer positions). PCR conditions for rtn4.1-A and rtn4.2-A (primers III + IV and VIII + IX, respectively) were 94 °C for 30 s, 76 °C for 30 s and 72 °C for 75 s (30 cycles). Different splice variants of rtn4.1-A and rtn4.2-A (1, 2 and 3) were amplified using the Expand Long Template PCR System (Roche Diagnostics, Mannheim, Germany) because PCR with Taq polymerase failed in this GC-rich sequence. This 'sensitive' PCR was performed with primers I + II and VI + VII, respectively, twice the amount of cDNA (2 μl) and the following cycling parameters: 92 °C for 10 s, 66 °C for 10 s, 68 °C for 40 s (24 cycles), 92 °C for 10 s, 66 °C for 10 s, 68 °C for 40 + 1 s/cycle (15 cycles).

Rtn4.1-B and rtn4.2-B splice variants were amplified using primer combinations I + V and VI + X, respectively (92 °C for 10 s, 63 °C for 10 s, 68 °C for 23 s (20 cycles), 92 °C for 10 s, 63 °C for 10 s, 68 °C for 23 + 1 s/cycle (15 cycles)). The short elongation time excluded amplification of A-splice variants in the same PCR reaction. All alternative splice products were subcloned into pCRII-TOPO vector and confirmed by sequencing.

Conditions for rtn4.1-C and rtn4.2-C (standard PCR; primers XI + XII and XI + XV, respectively) were 94 °C for 20 s, 63 °C for 15 s and 72 °C for 40 s (35 cycles). Rtn4.1-N was amplified using primer combination XIII + XII and standard PCR (94 °C for 20 s, 65 °C for 15 s and 72 °C for 45 s; 35 cycles). For rtn4.2-N detection, the AccuPrime System together with primers XIV + XV was applied (94 °C for 20 s, 63 °C for 15 s and 68 °C for 45 s; 35 cycles).

For each primer combination, positive and negative control PCRs on rtn4.1 and -2 plasmid DNA were included to prove specificity for one of the two genes. All PCRs were performed at least in duplicate, analysed on 1.5% (w/v) agarose gels and documented with a Molecular Imager FX (Bio-Rad, München, Germany).

Oligodendrocyte cultures

Tectum opticum and spinal cord of anesthetized postmetamorphic froglets were dissected in L-15 medium (Invitrogen) and the meninges and peripheral nerve roots were removed. The tissue was chopped with a McIlwain tissue chopper (Vibratome, St. Louis MO, USA) and the fragments were rinsed twice in L-15 containing 10% (v/v) fetal calf serum (FCS, Invitrogen). After centrifugation, the tissue was resuspended in 80% (v/v) DMEM/Ham's F-12 1:1, containing 10% (v/v) FCS, 0.4% (w/v) methyl-cellulose, 15 mM HEPES, 3.5 mg/ml glucose, 0.1 mg/ml glutamine, 5×10^{-3} mg/ml insuline, 0.1 mM putrescine, 2×10^{-5} mM progesterone, 3×10^{-5} mM sodium-selenite (all Sigma-Aldrich) and 0.05 mg/ml genta-

micine (Invitrogen) and plated on polylysine/laminin-coated coverslips (Bastmeyer et al., 1989). Cultures were further treated as described by Lang et al. (1995). Differentiated oligodendrocytes were obtained by adding 10 μM Forskolin (Biomol GmbH, Hamburg, Germany) to the culture medium.

Antibodies

For the generation of antisera AS702 and AS706, two different regions of the (XENLA)rtn4.1-A sequence (for details see Fig. 1) were cloned into pTrcHis expression vector (Invitrogen) and recombinantly expressed in Top 10F′ *E. coli* after IPTG induction. His-tagged proteins were purified under denaturing conditions on Ni^{+}-NTA spin columns (Qiagen) according to the manufacturer. Eluted protein (500 μl) was mixed with adjuvant (500 μl MPL + TDM + CWS, No. M6661, Sigma-Aldrich) and injected into rabbits every second week for five times. IgG fractions were isolated via a Protein A affinity chromatography (Amersham Biosciences) according to standard protocols. Specificity of AS702 and AS706 was increased by pre-absorption against general *E. coli* and unrelated His-tagged proteins. Proteins 833 (RTN4.1) and 834 (RTN4.2) were similarly expressed and purified to test specificity of AS702 and AS706.

Antibodies were used as follows: AS702 and AS706 against *Xenopus* Nogo-A/RTN4-A at 1:1000 for immunohistochemistry on tissue sections and at 1:10,000 for western blotting; AS 472 against rat Nogo-A (aa 623–640, affinity purified) at 1:10,000; monoclonal antibody (mAb) Olig hybridoma supernatant against oligodendrocytes/myelin (Steen et al., 1989) at 1:2 and mAb IN-1 hybridoma supernatant (Caroni and Schwab, 1988a) undiluted. Secondary antibodies were Cy3-conjugated donkey anti-rabbit IgG; HRP-conjugated goat anti-rabbit IgG (Jackson ImmunoResearch West Grove PA, USA), Alexa 488-conjugated goat anti-mouse IgG (Molecular Probes, Eugene OR, USA) and biotin-conjugated goat anti-mouse IgM (μ-chain specific; Vector Laboratories, Burlingame CA, USA).

Immunohistochemistry

For AS702, AS706 and IN-1 staining, isolated brains, spinal cords and retinae with optic nerves of stage 66 *X. laevis* were embedded in TissueTek (Sakura Finetek, Zoeterwoude, The Netherlands) and frozen in liquid nitrogen. Sections (12 μm) were cut on a cryostat (Leica, Bensheim, Germany), collected on SuperFrost Plus glass slides (Menzel-Glaser, Freiburg, Germany), fixed in Clark's solution (95% (v/v) ethanol/5% (v/v) acetic acid; 25 min at 4°C), rehydrated in 70% (v/v) ethanol (10 min at 4°C) and rinsed in PBS. Alternatively, tissues were fixed in 2% (w/v) PFA (overnight at 4°C), washed in PBS, transferred into a 20% (w/v) sucrose solution (overnight at 4°C) and embedded in TissueTek before sectioning. PFA-fixed sections were stained with AS702, AS706 or the myelin marker Olig. For Olig staining, 0.1% (v/v) Triton X-100 (Sigma-Aldrich) was added to the antibody solution.

Sections were incubated with primary antibodies (overnight at 4°C), rinsed in PBS, incubated with appropriate secondary antibodies (either Cy3-conjugated or biotinylated antibodies together with ABC and DAB kits (Vector Laboratories; 1 h at RT), rinsed and coverslipped with Mowiol (Merck Biosciences, Schwalbach, Germany) containing n-propyl gallate (Sigma-Aldrich).

Cultured oligodendrocytes were fixed in methanol (−20°C, 5 min), rinsed in PBS, incubated with AS706 overnight at 4°C, rinsed in PBS, incubated with Cy3-conjugated secondary antibody plus 50 ng/ml DAPI (4′ ,6′ -Diamidino-2-Phenylindole; Sigma-Aldrich) for 1 h at RT, rinsed and coverslipped with Mowiol. For blocking experiments, AS706 was preincubated with 0.45 mg/ml recombinant protein 706 for 1 h at 4°C before staining.

Gel electrophoresis and immunoblotting

X. laevis tissues were homogenized, separated on NewPAGE® Novex® 3–8% high resolution gradient tris-acetate gels (Invitrogen) and transferred to Hybond C Super nitrocellulose membranes (Amersham Biosciences) in a tank blot apparatus. For immunodetection, the membranes were incubated in blocking solution (3% (w/v) milk powder/0.05% (v/v) Tween 20/350 mM NaCl in PBS) at RT for at least 30 min. Primary antibody was added overnight at 4°C. After three washes for 15 min each with washing buffer (350 mM NaCl/0.05% (v/v) Tween 20 in PBS), the membranes were incubated with HRP-coupled secondary antibody for 1–2 h at RT. After three washes (10 min each), the blots were developed using the ECL Detection Kit (Amersham Biosciences) or SuperSignal West Pico (Pierce, Bonn, Germany) and exposed to X-ray films (Hyperfilm-ECL; Amersham Biosciences).

Acknowledgments

C.A.O.S. was supported by the Deutsche Forschungsgemeinschaft (DFG), M.K. by the "Stiftung der Deutschen Wirtschaft für Qualifizierung und Kooperation e.V. (sdw)" T.O. and M.E.S. by the Swiss National Science Foundation (Grant No. 31-63633) and by the NCCR on Neural Plasticity and Repair. The hybridoma supernatant of the monoclonal antibody Olig (developed by M. Constantine-Paton) was obtained from the Developmental Studies Hybridoma Bank developed under auspices of the NICHD and maintained by the University of Iowa, Department of Biological Science. Iowa City, IA 52242. We thank U. Binkle for technical assistance and J. Taylor for critical reading of the manuscript.

References

Bastmeyer, M., Beckmann, M., Nona, S.M., Cronly-Dillon, J.R., Stuermer, C.A., 1989. Identification of astrocyte- and oligodendrocyte-like cells of goldfish optic nerves in culture. Neurosci. Lett. 101, 127–132.

Beattie, M.S., Bresnahan, J.C., Lopate, G., 1990. Metamorphosis alters the response to spinal cord transection in *Xenopus laevis* frogs. J. Neurobiol. 21, 1108–1122.

Caroni, P., Schwab, M.E., 1988a. Antibody against myelin-associated inhibitor of neurite growth neutralizes nonpermissive substrate properties of CNS white matter. Neuron 1, 85–96.

Caroni, P., Schwab, M.E., 1988b. Two membrane protein fractions from rat central myelin with inhibitory properties for neurite growth and fibroblast spreading. J. Cell Biol. 106, 1281–1288.

Chen, M.S., Huber, A.B., van der Haar, M.E., Frank, M., Schnell, L., Spillmann, A.A., Christ, F., Schwab, M.E., 2000. Nogo-A is a myelin-associated neurite outgrowth inhibitor and an antigen for monoclonal antibody IN-1. Nature 403, 434–439.

Clarke, J.D., Alexander, R., Holder, N., 1988. Regeneration of descending axons in the spinal cord of the axolotl. Neurosci. Lett. 89, 1–6.

Forehand, C.J., Farel, P.B., 1982. Anatomical and behavioral recovery from the effects of spinal cord transection: dependence on metamorphosis in anuran larvae. J. Neurosci. 2, 652–654.

Gaze, R.M., 1970. The Formation of Nerve Connections. Academic Press, New York.

GrandPré, T., Nakamura, F., Vartanian, T., Strittmatter, S.M., 2000. Identification of the Nogo inhibitor of axon regeneration as a Reticulon protein. Nature 403, 439–444.

Huber, A.B., Weinmann, O., Brosamle, C., Oertle, T., Schwab, M.E., 2002. Patterns of Nogo mRNA and protein expression in the developing and adult rat and after CNS lesions. J. Neurosci. 22, 3553–3567.

Hughes, M.K., Hughes, A.L., 1993. Evolution of duplicate genes in a tetraploid animal, *Xenopus laevis*. Mol. Biol. Evol. 10, 1360–1369.

Hunt, D., Coffin, R.S., Anderson, P.N., 2002a. The Nogo receptor, its ligands and axonal regeneration in the spinal cord; a review. J. Neurocytol. 31, 93–120.

Hunt, D., Mason, M.R., Campbell, G., Coffin, R., Anderson, P.N., 2002b. Nogo receptor mRNA expression in intact and regenerating CNS neurons. Mol. Cell. Neurosci. 20, 537–552.

Josephson, A., Widenfalk, J., Widmer, H.W., Olson, L., Spenger, C., 2001. NOGO mRNA expression in adult and fetal human and rat nervous tissue and in weight drop injury. Exp. Neurol. 169, 319–328.

Klinger, M., Diekmann, H., Haenisch, C., Oertle, T., Schwab, M.E., Stuermer, C.A.O., 2002. Cloning and characterization of zebrafish reticulon genes including nogo/RTN-4. Soc. Neurosci. Abst. 28 (Programm No. 333.314).

Kozak, M., 1996. Interpreting cDNA sequences: some insights from studies on translation. Mamm. Genome 7, 563–574.

Kumar, S., Tamura, K., Jakobsen, I.B., Nei, M., 2001. MEGA2: Molecular Evolutionary Genetics Analysis Software. Tempe, Arizona, USA.

Lang, D.M., Stuermer, C.A., 1996. Adaptive plasticity of *Xenopus* glial cells in vitro and after CNS fiber tract lesions in vivo. Glia 18, 92–106.

Lang, D.M., Rubin, B.P., Schwab, M.E., Stuermer, C.A., 1995. CNS myelin and oligodendrocytes of the *Xenopus* spinal cord—but not optic nerve—are nonpermissive for axon growth. J. Neurosci. 15, 99–109.

Li, W.H., Gouy, M., Sharp, P.M., O'Huigin, C., Yang, Y.W., 1990. Molecular phylogeny of Rodentia, Lagomorpha, Primates, Artiodactyla, and Carnivora and molecular clocks. Proc. Natl. Acad. Sci. U. S. A. 87, 6703–6707.

McKerracher, L., David, S., Jackson, D.L., Kottis, V., Dunn, R.J., Braun, P.E., 1994. Identification of myelin-associated glycoprotein as a major myelin-derived inhibitor of neurite growth. Neuron 13, 805–811.

Morgenstern, D.A., Asher, R.A., Fawcett, J.W., 2002. Chondroitin sulphate proteoglycans in the CNS injury response. Prog. Brain Res. 137, 313–332.

Nei, M., Gojobori, T., 1986. Simple methods for estimating the numbers of synonymous and nonsynonymous nucleotide substitutions. Mol. Biol. Evol. 3, 418–426.

Oertle, T., Schwab, M.E., 2003. Nogo and its paRTNers. Trends Cell Biol. 13, 187–194.

Oertle, T., Huber, C., van der Putten, H., Schwab, M.E., 2003a. Genomic structure and functional characterisation of the promoters of human and mouse nogo/rtn4. J. Mol. Biol. 325, 299–323.

Oertle, T., Klinger, M., Stuermer, C.A., Schwab, M.E., 2003b. A reticular rhapsody: phylogenic evolution and nomenclature of the RTN/Nogo gene family. FASEB J. 17, 1238–1247.

Oertle, T., Merkler, D., Schwab, M.E., 2003c. Do cancer cells die because of Nogo-B? Oncogene 22, 1390–1399.

Oertle, T., van der Haar, M.E., Bandtlow, C.E., Robeva, A., Burfeind, P., Buss, A., Huber, A.B., Simonen, M., Schnell, L., Brosamle, C., Kaupmann, K., Vallon, R., Schwab, M.E., 2003d. Nogo-A inhibits neurite outgrowth and cell spreading with three discrete regions. J. Neurosci. 23, 5393–5406.

Prinjha, R., Moore, S.E., Vinson, M., Blake, S., Morrow, R., Christie, G., Michalovich, D., Simmons, D.L., Walsh, F.S., 2000. Inhibitor of neurite outgrowth in humans. Nature 403, 383–384.

Spillmann, A.A., Bandtlow, C.E., Lottspeich, F., Keller, F., Schwab, M.E., 1998. Identification and characterization of a bovine neurite growth inhibitor (bNI-220). J. Biol. Chem. 273, 19283–19293.

Steen, P., Kalghatgi, L., Constantine-Paton, M., 1989. Monoclonal antibody markers for amphibian oligodendrocytes and neurons. J. Comp. Neurol. 289, 467–480.

Van de Peer, Y., Taylor, J.S., Braasch, I., Meyer, A., 2001. The ghost of selection past: rates of evolution and functional divergence of anciently duplicated genes. J. Mol. Evol. 53, 436–446.

van de Velde, H.J., Roebroek, A.J., Senden, N.H., Ramaekers, F.C., Van de Ven, W.J., 1994. NSP-encoded reticulons, neuroendocrine proteins of a novel gene family associated with membranes of the endoplasmic reticulum. J. Cell Sci. 107, 2403–2416.

Wang, K.C., Koprivica, V., Kim, J.A., Sivasankaran, R., Guo, Y., Neve, R.L., He, Z., 2002a. Oligodendrocyte-myelin glycoprotein is a Nogo receptor ligand that inhibits neurite outgrowth. Nature 417, 941–944.

Wang, X., Chun, S.J., Treloar, H., Vartanian, T., Greer, C.A., Strittmatter, S.M., 2002b. Localization of Nogo-A and Nogo-66 receptor proteins at sites of axon-myelin and synaptic contact. J. Neurosci. 22, 5505–5515.

Zhou, Z.M., Sha, J.H., Li, J.M., Lin, M., Zhu, H., Zhou, Y.D., Wang, L.R., Wang, Y.Q., Zhou, K.Y., 2002. Expression of a novel reticulon-like gene in human testis. Reproduction 123, 227–234.